RSC Advances

ROYAL SOCIETY OF CHEMISTRY

www.rsc.org/advances

Cite this: DOI: 10.1039/c0xx00000x

www.rsc.org/xxxxxx

ARTICLE TYPE

Phosphate-containing Metabolites Switch on Phosphorescence of Ferric Ions Engineered Carbon Dots in Aqueous Solution†

Jin-Long Chen,[ab1] Xiao Yan,[a1] Meng-Xiang, Su,[ab] Fang Yan[ab], Bo Li[ab] and Bin Di*[ab]

Received (in XXX, XXX) Xth XXXXXXXXX 20XX, Accepted Xth XXXXXXXXX 20XX

DOI: 10.1039/b000000x

While most research works focus on the development of carbon dots (CDs)-based fluorescence sensors, much less attention is paid to phosphorescence phenomenon and their potential applications to date. Herein, room temperature phosphorescence (RTP) of water-soluble CDs free of deoxidants and other inducers was firstly observed in pure aqueous solution in this work. RTP of CDs could be significantly quenched when chelating with iron ions as well as aggregation of CDs, presumably resulting from the effective electron transfer process between CDs and iron ions. Due to a high affinity of iron ions to phosphate ions through well-known Fe–O–P bonds, the quenched RTP of functionalized CDs by Fe^{3+} could be basically recovered in the presence of phosphate-containing molecules. For a proof-of-concept demonstration, adenosine-5'-triphosphate (ATP), as a predominant phosphate-containing metabolite was quantitatively detected by a phosphorescence "off-to-on" approach. The enhancement of RTP at 440 nm was linearly proportional to the concentrations of ATP ranging from 20 to 200 μM with a detection limit as low as 14 μM. Moreover, the conducted iron ions engineered CDs based RTP probe was explored to estimate ATP levels in human blood plasma.

Introduction

Carbon dots (CDs) have attracted much attention in recent year, owing to advantages such as excellent optical properties, low toxicity, good biocompatibility, hydrophilicity and simple synthesis.[1-4] While most researches focus on the development of CDs based on fluorescence, the phosphorescence property has been paid much less attention. Room temperature phosphorescence (RTP) has been increasingly applied in sensing, bio-imaging and anti-counterfeiting.[5-7]On account of the emission delay, phosphorescence detection possesses a significant superiority that any fluorescence emission and scattering light could be refrained simply. In addition, only a very few number of compounds are able to emit analytically useful phosphorescence at room temperature.[8] As is well known, RTP was generally originated from inorganics or metal complexes which may represent serious limitation with the known toxicity, potential environment hazard and costliness.[9-11] RTP emitted by CDs, until now, has been observed only in assistant with the perturbation of heavy atom, or onto solid support.[12, 5] However, RTP emission from CDs dispersed in water medium has not been reported before. Interestingly, we have found that phosphorescence emission can be observed in the water dispersing CDs at room temperature.

Phosphate-containing metabolites, which include nucleoside pyrophosphates, pyrophosphates, phosphates and phosphoproteins, play critical roles in biological processes.[13]The level of phosphate-containing metabolites can be used as an indication of the orderly condition of biological systems. For example, adenosine-5'-triphosphate (ATP), an extracellular signaling agent and the major energy carrier in cells, which has not only been used as an indicator of cell viability, but also associated with particular diseases such as angiocardiopathy due to excessive production of ATP by creatine kinase.[14-16] In general, the physiologic concentration of blood phosphoate is at millimolar level, which is mainly dominated by ATP.[17] Although the traditional determination of ATP levels in vitro such as luciferase assay, is sensitive, the enzyme and substrates are costly and of uncertain stability.[18] Considerable efforts have been devoted in designing fluorescence probe to detect phosphorylated species, but the fluorescence method might be interfered by the scattering light or the fluorescence from matrixes.[19-21]

Herein, we firstly demonstrate a phosphorescence "off-to-on" approach to sensing ATP by utilization of functionalized CDs. The phosphorescence of CDs is significantly quenched when chelating with iron ions, then "turn-on" in present of phosphorylated species. Since ATP is the main phosphate-containing metabolites in plasma, the proposed sensing assay can

[a]*Department of Pharmaceutical Analysis, China Pharmaceutical University, Nanjing 210009, China. Fax: +86 2583271269; Tel: +86 2593271269; Email: dibin@cpu.edu.cn; ddw888@vip.sina.com*

[b]*Key Laboratory of Drug Quality Control and Pharmacovigilance (China Pharmaceutical University), Ministry of Education, Nanjing 210009, China*

[1]*Jin-Long Chen and Xiao Yan contributed equally to this work*

†Electronic supplementary information (ESI) available. See DOI: 10.1039/b000000x/

be successfully used to rapidly estimate the levels of phosphate-containing metabolites in plasma.

Experimental section

Materials and apparatus

Citric acid, ethylenediamine, ferric trichloride hexahydrate ($FeCl_3 \cdot 6H_2O$), tris(hydroxymethyl)aminomethane were of analytical grade and used without further purification. Adenosine 5'-triphosphate (ATP) disodium trihydrate was purchased from Sigma-Aldrich and kept in the freezer under -20 °C. Human blood plasma was kindly provided by China Pharmaceutical University Hospital Department. All aqueous solutions were prepared with deionized water purified through PL5242 Purelab Classic UV (PALL Co. Ltd., USA) to a resistivity of 18.2 MΩ·cm.

Instrumentation

Phosphorescence measurements were performed on a Hitachi F-4600 spectrofluorometer (Hitachi Co. Ltd., Japan) in phosphorescence mode. Transmission electron microscopy (TEM) images were obtained from a TECNAI G2 F20 (FEI Co., USA). UV-Vis absorption spectra were recorded with a Shimadzu UV-2401 PC instrument (Shimadzu Co. Ltd., Japan). The FT-IR spectra (4000-400 cm-1) in KBr were collected on a Jasco FT-IR-4100 spectrometer (Jasco Co. Ltd., Japan). Time-resolved fluorescence and phosphorescence decay by delay were performed on a FluoroMax-4 spectrofluorometer (Horiba Jobin Yvon Co. Ltd., France).

Preparation of Phosphorescent CDs

Modifying from the previous work, [22] 0.42 g of citric acid and 535 μL of ethylenediamine were dissolved in 10 mL of deionized water. Then the solution was transferred to a Teflon-lined stainless autoclave and heated at 200 °C for 5 hours. Cool the reactor to room temperature, the resultant CDs solution was purified by silica gel column with water as the developing solvent. The purified CDs solution was freeze-dried under vaccum. Finally, the brown-black hygroscopic CDs were obtained and stored in a dark desiccator at room temperature.

Phosphorescence measurement

The "on-off-on" alternation of the phosphorescence of CDs was performed in the Tris-HCl buffer at pH 8.0. To a 5.00 mL volumetric flask, 1 mL of 10.0 mM Tris-HCl buffer, 250 μL of 1 mg mL^{-1} aqueous CDs and 250 μL of 10.0 mM aqueous $FeCl_3$ were sequentially added. After 5 min incubation at room temperature, an appropriate volume of stock ATP solution was added into the mixture to make the desired concentrations. The mixture was diluted with deionized water to the volume, mixed well and then incubated for 30 min at room temperature. Subsequently, the phosphorescence intensity of the solution was measured at $\lambda_{em}/\lambda_{ex}$= 440/360 nm.

Determination of ATP in human blood plasma

Acetonitrile was by first added to equal volume of human blood plasma for protein precipitation. The mixture was centrifuged at 5,000 rpm for 5 minutes and the supernatant was collected. ATP was spiked into the aliquots supernatant and then the mixture was diluted to a particular volume to make the 10-fold diluted human blood plasma that contains different concentrations of spiked ATP. Aliquots of ATP spiked 10-fold diluted human blood plasma (500 μL) were then processed with the aforementioned sensing procedure. Subsequently, the phosphorescence spectra were recorded.

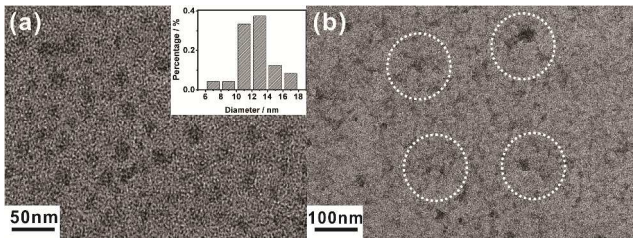

Fig. 1 TEM images of (a) CDs alone, the inset shows the size distribution of CDs. and (b) CDs-Fe^{3+}, apparent aggregation of CDs in white dotted circle.

Results and discussion

Morphological and Structural Characterizations of CDs

The CDs were prepared by use of a facile hydrothermal method. The reaction was conducted by first condensing citric acid and ethylenediamine at 200 °C for 5 hours, whereupon they formed polymer-like CDs, which were then carbonized to form the CDs. The morphology and structure of CDs were confirmed by analysis described as followings. The transmission electron microscopy (TEM) images (Fig. 1a) reveal the homogeneous CDs with spherical shape and almost uniform size in diameter about 11.5 nm. Fig. 1b also reveals the apparent aggregation of CDs induced by Fe^{3+} ions, suggesting that CDs formed chelation with Fe^{3+}, thereby quenching the phosphorescence. As seen from the FT-IR spectrum (Fig. S1 in the ESI†) that stretching vibrations of C-OH at 3430 cm^{-1} , C-H at 2923 cm^{-1}, 2850 cm^{-1}, 1476 cm^{-1} and a broad peak at 1570 cm^{-1} originate from vibrations of aromatic C=C, asymmetric stretching vibrations of C-NH-C at 1126 cm^{-1}, bending vibrations of N-H at 1570 cm^{-1}, and the vibrational absorption band of C=O at 1635 cm^{-1} suggest those CDs produced by citric acid and ethylenediamine containing C=C, C=O, -OH, -NH and -CH groups.

Phosphorescence properties of CDs

The CDs were produced from condensing citric acid and ethylenediamine by use of a facile hydrothermal method under different conditions in this work. As shown in Fig. 2 and Fig.5d, the obtained CDs displayed a highly strong photoluminescence including fluorescence with a short lifetime of 14.4 ns and phosphorescence with a long lifetime of 160 μs. Excitation/solvent -dependent emission behaviour (Fig. S2 in the ESI†) was observed, which is common in fluorescent carbon-containing nanoparticles related with the surface state. In careful comparison to fluorescence characteristics, we found that phosphorescence emission profile of CDs displayed only an enhancement in the longer wavelength region (500-600 nm) without new emission band shifted to a long wavelength, similar to that of Mn doped ZnS quantum dots.[6] As demonstrated in the UV-Vis absorption spectrum (Fig. 2d), the peak centred at 240 nm is attributed to π-π* transition of C=C, and the peak at 350 nm

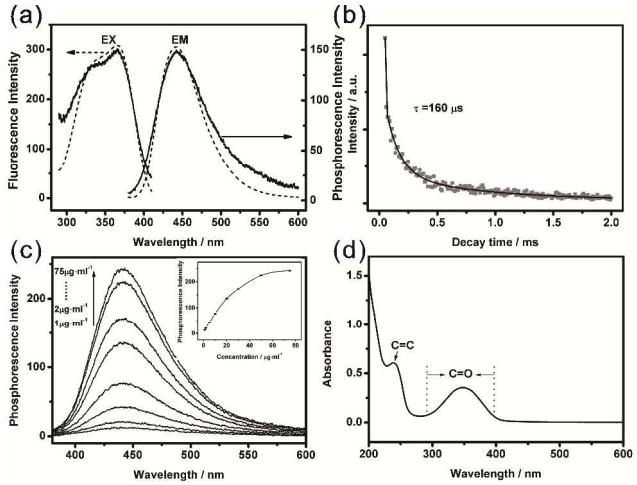

Fig. 2 (a) Phosphorescence spectra (solid line) and fluorescence spectra (dash line) of CDs. (b) Time resolved phosphorescence decay by delay of CDs. (c) RTP emission profiles of different concentrations of CDs. (d) The UV-Vis absorption spectrum of CDs dispersed in water.

is attributed to the *n*-π* transition of C=O. With the emission at 440 nm, the phosphorescence excitation spectrum performs a broad band from 300 to 400 nm and overlaps the band of C=O, suggesting that the phosphorescence may come from the C=O bonds on carbon dots. In addition, as to aromatic carbonyl group, the singlet and triplet states of aromatic carbonyl group are close in energy, and the spin-orbit coupling is efficient, so that it is prone to intersystem crossing.[5] Therefore, it is reasonable to suppose that the phosphorescence originates from the aromatic carbonyl group on CDs. Moreover, it is well known that polycyclic aromatic hydrocarbons are family of compounds which can be directly determined by room temperature phosphorimetry.[8]The phosphorescence of CDs also possibly related with the graphitic structure which is similar to the polycyclic aromatic structure. Along with a serial of representative RTP emission spectra at different concentrations of CDs in water, no emission wavelength shift was observed even at the lowest concentration. A plot of the dependence of integrated RTP intensity version nanoparticles concentration (or dilution factor) with a good linear relationship was shown in inset in Fig. 2c. This exhibited that CDs were equably dispersed in water in a large concentration range. Substantial phosphorescence integrated intensities with good signal-to-noise ratios and well-resolved emission spectrum smaller than 1 μg of particles per liter. Furthermore, a series of CDs samples were collected under different reaction temperatures and ratios of precursors. Results showed that reaction temperature gave a significant effect on the phosphorescence intensity, while ratio of precursors had a slight effect (Fig. S3 in the ESI†). It is worthy to be noted that the photophysical characteristics described above is different from the common organic small molecules. The corresponding clear-cut phosphorescence mechanism need to be further studied in the future. The above results of the synthetic CDs with high stability and high luminescence quantum yield in aqueous solution were in favour of phosphorescence sensing and detection.

Effects of pH on the sensing of ATP

The effects of pH on the phosphorescence intensity of CDs sensing system were investigated (Fig. 3). Phosphorescence

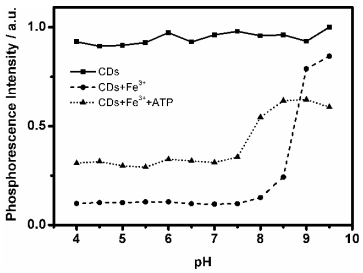

Fig.3 Effect of pH on the phosphorescence intensity of CDs (50 μg mL^{-1}) only, CDs (50 μg mL^{-1}) + Fe^{3+} (500 μM) and CDs (50 μg mL^{-1}) + Fe^{3+} (50 μM) + ATP (1200 μM), respectively.

intensities of CDs only remain nearly constant in a wide range of pH from 4.0 to 9.5 without changes in RTP emission profile. The mixture solution of CDs and iron ions was observed with the naked-eye. Apparent precipitations occurred at pH higher than 8.0 due to its hydrolysis, accompanied with the weakness of the quenching capacity of Fe^{3+}. However, for ATP sensing, larger phosphorescence recovery could be obtained at higher pH. In view of a comprehensive consideration of sensitivity and reproducibility, a 10 mM Tris-HCl buffer of pH 8.0 was recommended to be used throughout.

Selectivity of the CDs-based phosphorescence method

The considerable phosphorescence of the CDs was found to be selectively quenched in the presence of Fe^{3+} as shown in Fig.S4a (in the ESI†).[22] In addition, the effects of a various of other metal ions were investigated including K^+, Na^+, Li^+, Ca^{2+}, Mg^{2+}, Mn^{2+}, Ba^{2+}, Cu^{2+}, Pb^{2+}, Ag^+, Zn^{2+}, Cd^{2+}, Co^{2+}, Ni^{2+} and Fe^{2+}. As shown in Fig. 4a, only Fe^{3+} brought the marked phosphorescence quenching. The phosphorescence of CDs gradually decreased when increased the concentration of Fe^{3+} ions. The quenching effect presumably results from the effective electron transfer that occurs from carboxyl and hydroxyl groups functionalized CDs complexation with Fe^{3+}. Besides, it is widely known that phosphate ions gave a considerable affinity to iron ions through Fe-O-P bonds.[21, 23]

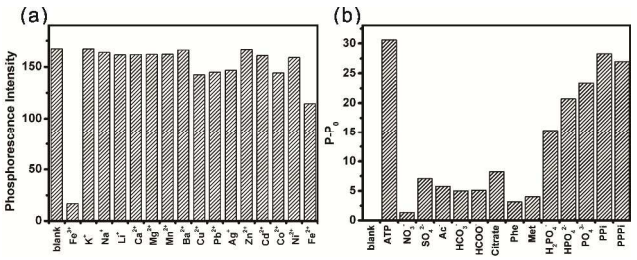

Fig. 4 (a) Phosphorescence intensity of CDs (50 μg mL^{-1}) after addition of different metal ions (500 μM). (b) Phosphorescence enhancement of CDs (50 μg mL^{-1})-Fe^{3+}(500 μM) system up addition of different anions (100 μM). P and P_0 are phosphorescence intensity with and without anions, respectively.

Therefore, the quenching phosphorescence of CDs caused by Fe^{3+} can be recovered in the presence of phosphate-containing molecules. Hence, we further evaluated the selectivity of the "off-on" phosphorescence approach to familiar anions such as NO_3^-, SO_4^{2-}, Ac^-, HCO_3^-, formate, citrate, phenylalanine, methionie, $H_2PO_4^-$, HPO_4^{2-}, PO_4^{3-}, pyrophosphate and tripolyphosphate. As indicated in the Fig. 4b, ATP has the greatest effect on the restoration of the phosphorescence that quenched by Fe^{3+}.

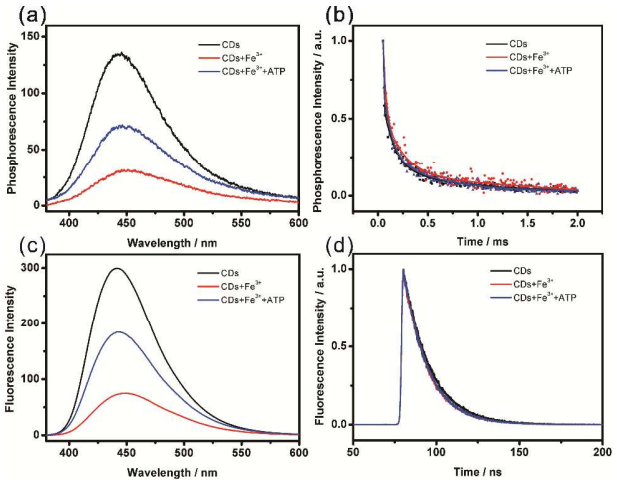

Fig. 5 (a) State phosphorescence spectra and time-resolved phosphorescence decay (b) of CDs alone, CDs+Fe^{3+}, and CDs+Fe^{3+} +ATP; (c) State fluorescence spectra and time-resolved fluorescence decay (d) of CDs alone, CDs+Fe^{3+}, and CDs+Fe^{3+} +ATP.

Moreover, it is notable that multiphosphates show higher affinity to Fe^{3+} than monophosphates (Fig. S5 in the ESI†).

Incubation time and time-resolved phosphorescence decay assays

To evaluate the effect of incubation time, the phosphorescence intensity as a function of time was monitored. As illustrated in Fig. S6 (in the ESI†), the chelation between CDs and Fe^{3+} was a quite rapid process that reached equilibrium in 5 min. While the formation and release of the ATP-Fe^{3+} complex from CDs was relatively slow and achieved equilibrium in almost 30 min. As seen from Fig. S4b (in the ESI†) that the linear relationship between (P_0-P) and concentration of Fe^{3+} ions shows that the phosphorescence quenching follows the Lineweaver-Burk Equation well, while the relationship between P_0/P and the concentration of Fe^{3+} does not follow Stern-Volmer's Equation. Thus, it is reasonable to suppose that RTP of CDs quenched by Fe^{3+} ions was in agreement with a static quenching model. To better understand the RTP "off-to-on" mechanism for sensing ATP, time-resolved phosphorescence and fluorescence decay of CDs in presence of Fe^{3+} and ATP were studied, respectively. Decay profiles are shown in Fig. 5. The phosphorescence lifetime of free CDs is about 160 μs, while a slight increment of lifetime of 166 μs was observed in the presence of Fe^{3+} ions, and the subsequent addition of ATP, with a lifetime of 159 μs. A similar trend has also been observed time-resolved fluorescence decay profile. These results described above suggested that the phosphorescence quenching mechanism of CDs by Fe^{3+} was attributed to a static quenching process resulting from effective electron transfer from photoinduced excited electron-hole pair of CDs to irons ions, and then Fe^{3+} dissociated from CDs by the phosphate species through the strong interactions.

Sensitivity of the sensing system

To demonstrate that the present system can be applied in sensing of ATP, the phosphorescence responses to ATP at different concentrations were measured under optimum conditions. The phosphorescence emission spectra of the system upon the addition of different concentrations of ATP ranging from 20 to

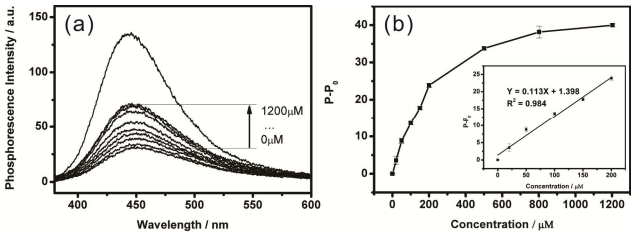

Fig. 6 (a) Phosphorescence emission spectra of CDs-Fe^{3+} (50 μg mL^{-1}-500 μM) in the presence of different concentrations of ATP (0, 20, 50, 100, 150, 200, 500, 800, 1200 μM). (b) The relationship between (P-P_0) and the concentration of ATP. P and P_0 are phosphorescence intensity with and without ATP, respectively.

1200 μM were shown in the Fig. 6a. Fig. 6b shows a dramatic increment of the phosphorescence intensity as the concentration of ATP increased. Meanwhile, inset of Fig. 6b clearly illustrates the corresponding calibration curve plot between the phosphorescence intensity enhancement factors (P-P_0) against the ATP concentration. The linear working concentration range was found to be 20-200 μM. The regression equation is Y= 0.113X+1.398, with correlation coefficient (R^2) of 0.994. Moreover, the limit of detection (LOD) was estimated to be 14 μM (3σ/S), in which σ is the standard deviation for the blank solution (n= 6), and S is the slope of the calibration curve.

Measuring ATP in real blood plasma samples

In order to evaluate the applicability of the proposed CDs based RTP "off-to-on" sensing approach, ATP assay in real human blood plasma sample was further studied. As shown in the Fig. 7a, the fluorescent background of blood plasma was significant (black line), while no background was observed in the phosphorescence mode (red line). Since only a very few number of species are able to emit analytically useful phosphorescence at room temperature,[8] the long delay time of phosphorescence can simply avoid the interferences of the scattering light and the undesired fluorescence emission.

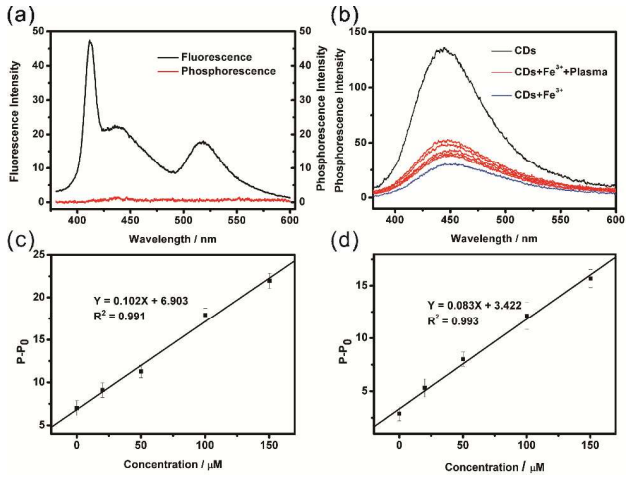

Fig. 7 (a) RTP (red line) and fluorescence (black line) spectra of human blood plasma. (b) Representative phosphorescence emission spectra of CDs (50 μg mL^{-1})-Fe^{3+}(500 μM) in the presence of 100-fold diluted human blood plasma spiked with different concentrations of ATP (0, 20, 50, 100 and 150 μM). (c, d) The corresponding relationship between (P-P_0) and the concentration of spiked ATP in the two human blood plasma samples.

A standard addition method was applied to estimate the ATP

concentration in human blood plasma. Different concentrations of ATP were spiked into the 10-fold diluted human blood plasma and were further incubated with the CDs-Fe^{3+} sensing system under the optimal conditions. In the test solution, human blood plasma was finally 100-fold diluted and the spiked ATP were at concentration of 0, 20, 50, 100, 150 μM. The blood plasma samples from 2 healthy volunteers were measured and the results are shown in the Fig. 7b. It was found that the present approach provides a linear response to ATP spiked into human blood plasma, and the regression equations are Y= 0.102X+ 6.903 and Y= 0.083X + 3.422, with the correlation coefficients (R^2) of 0.991 and 0.993 respectively (Fig.7c and Fig.7d). Using the standard addition method, we estimated that the concentrations of ATP of the 2 human blood plasma samples are 6.77 mM and 4.07 mM respectively. As previously mentioned, the physiologic concentration of blood phosphates is at millimolar level, which is mainly dominated by ATP. Thus we considered that ATP was mainly responsible for the phosphorescence recovery in the sensing process. Consequently, the proposed sensing system can be used to evaluate the health conditions of individuals.

Conclusions

In summary, we have demonstrated a novel RTP method based on the phosphorescence property of CDs for the cost-effective, readily, sensitive detection of ATP, a main phosphate-containing metabolite in human blood plasma. The phosphorescence emission centred at 440 nm with an average lifetime of 160 μs under excitation of 360 nm can be quenched in present of Fe^{3+} attributing to nonradiative electron transfer and then turned on by the phosphate ions through the strong interactions. Deoxidants and other inducers that are necessary in conventional RTP detection and interferences from autofluorescence and the scattering light of the complex matrix encountered in spectrofluorometry could be readily avoided in the present CDs-based RTP. Combination of varieties of interactions between metal ions and surface ligands of CDs and the desirable phosphorescence properties show that water-soluble and biocompatible CDs are promising for RTP chemical and biological sensing and time-resolved imaging. Moreover, CDs-based RTP nanocomposites could potentially be used in anti-counterfeiting, especially for food and drugs.

Acknowledgement

The authors gratefully acknowledge the financial support for this work from the National Natural Science Foundation of China (Grant No. 21305161), the Natural Science Foundation of Jiangsu Province (Grant No. BK20130643).

Notes and references

1 C. Q. Ding, A.W. Zhu and Y. Tian, *Acc. Chem. Res*., 2013, **47**, 20-30.
2 Y. P. Sun, B. Zhou, Y. Lin, W. Wang, K. A. Fernando, P. Pathak, M. J. Meziani, B. A. Harruff, X. Wang, H. Wang, P. G. Luo, H. Yang, M. E. Kose, B. Chen, L. M. Veca and S. Y. Xie, *J. Am. Chem. Soc*., 2006, **128**, 7756-7757.
3 H. Ding, L. W. Cheng, Y. Y. Ma, J. L. Kong and H. M. Xiong, *New J. Chem*., 2013, **37**, 2515-2520.
4 K. G. Qu, J. S. Wang, J. S. Ren and X. G. Qu, *Chemistry*, 2013, **19**, 7243-7249.
5 Y. Deng, D. Zhao, X. Chen, F. Wang, H. Song and D. Shen, *Chem. Commun.*, 2013, **49**, 5751-5753.
6 Y. He, H. F. Wang and X. P. Yan, *Anal. Chem.*, 2008, **80**, 3832-3837.
7 Q. Zhao, C. Huang and F. Li, *Chem. Soc. Rev.*, 2011, **40**, 2508-2524.
8 A. Salinas Castillo, A. Segura Carretero, J. Costa Fernández, W. J. Jin and A. Fernández Gutiérrez, *Anal. Chim. Acta*, 2004, **516**, 213-220
9 E. Sotelo-Gonzalez, L. Roces, S. Garcia-Granda, M. T. Fernandez-Arguelles, J. M. Costa-Fernandez and A. Sanz-Medel, *Nanoscale*, 2013, **5**, 9156-9161.
10 X. J. Mao, H. Z. Zheng, Y. J. Long, J. Du, J. Y. Hao, L. L. Wang and D. B. Zhou, *Spectrochim. Acta. A*, 2010, **75**, 553-557.
11 X. Michalet, F. F. Pinaud, L. A. Bentolila, J. M. Tsay, S. Doose, J. J. Li, G. Sundaresan, A. M. Wu, S. S. Gambhir and S. Weiss, *Science*, 2005, **307**, 538-544.
12 L. P. Lin, X. X. Wang, S. Q. Lin, L. H. Zhang, C. Q. Lin, Z. M. Li and J. M. Liu, *Spectrochim. Acta. A*, 2012, **95**, 555-561.
13 G. V. Zyryanov, M. A. Palacios and P. Anzenbacher, *Angew. Chem. Int. Edit.*, 2007, **46**, 7849-7852.
14 J. R. Knowles, *Annu. Rev. Biochem.*, 1980, **49**, 877-919.
15 F. Liu, J. Zhang, R. Chen, L. Chen and L. Deng, *Chem. Biodivers.*, 2011, **8**, 311-316.
16 N. Azorin, M. Raoux, L. Rodat-Despoix, T. Merrot, P. Delmas and M. Crest, *Exp. Dermatol.*, 2011, **20**, 401-407.
17 P. H. Li, J. Y. Lin, C. T. Chen, W. R. Ciou, P. H. Chan, L. Luo, H. Y. Hsu, E. W. G. Diau and Y. C. Chen, *Anal. Chem.*, 2012, **84**, 5484-5488
18 W. Tedsana, T. Tuntulani and W. Ngeontae, *Anal. Chim. Acta*, 2013, **783**, 65-73.
19 H. N. Lee, Z. Xu, S. K. Kim, K. M. K. Swamy, Y. Kim, S. J. Kim and J. Yoon, *J. Am. Chem. Soc.*, 2007, **129**, 3828-3829.
20 L. N. Zhong, F. F. Xing, Y. L. Bai, Y. M. Zhao and S. R. Zhu, *Spectrochim. Acta. A*, 2013, **115**, 370-375.
21 J. J. Liu, X. L. Zhang, Z. X. Cong, Z. T. Chen, H. H. Yang and G. N. Chen, *Nanoscale*, 2013, **5**, 1810-1815.
22 S. J. Zhu, Q. N. Meng, L. Wang, J. H. Zhang, Y. B. Song, H. Jin, K. Zhang, H. C. Sun, H. Y. Wang and B. Yang, *Angew. Chem.*, 2013, **52**, 3953-3957.
23 J. A. Simmons, *Water, Air, Soil Pollut.*, 2010, **209**, 123-132.

Figure legends

Fig. 1 TEM images of (a) CDs alone, the inset shows the size distribution of CDs. and (b) CDs-Fe^{3+}, apparent aggregation of CDs in white dotted circle.

Fig. 2 (a) Phosphorescence spectra (solid line) and fluorescence spectra (dash line) of CDs. (b) Time resolved phosphorescence decay by delay of CDs. (c) RTP emission profiles of different concentrations of CDs. (d) The UV-Vis absorption spectrum of CDs dispersed in water.

Fig.3 Effect of pH on the phosphorescence intensity of CDs (50 μg mL^{-1}) only, CDs (50 μg mL^{-1}) + Fe^{3+} (500 μM) and CDs (50 μg mL^{-1}) + Fe^{3+} (50 μM) + ATP (1200 μM), respectively.

Fig. 4 (a) Phosphorescence intensity of CDs (50 μg mL^{-1}) after addition of different metal ions (500 μM). (b) Phosphorescence enhancement of CDs (50 μg mL^{-1})-Fe^{3+}(500 μM) system up addition of different anions (100 μM). P and P_0 are phosphorescence intensity with and without anions, respectively.

Fig. 5 (a) State phosphorescence spectra and time-resolved phosphorescence decay (b) of CDs alone, CDs+Fe^{3+}, and CDs+Fe^{3+} +ATP; (c) State fluorescence spectra and time-resolved fluorescence decay (d) of CDs alone, CDs+Fe^{3+}, and CDs+Fe^{3+} +ATP.

Fig. 6 (a) Phosphorescence emission spectra of CDs-Fe^{3+} (50 μg mL^{-1}-500 μM) in the presence of different concentrations of ATP (0, 20, 50, 100, 150, 200, 500, 800, 1200 μM). (b) The relationship between (P-P_0) and the concentration of ATP. P and P_0 are phosphorescence intensity with and without ATP, respectively.

Fig. 7 (a) RTP (red line) and fluorescence (black line) spectra of human blood plasma. (b) Representative phosphorescence emission spectra of CDs (50 μg mL^{-1})-Fe^{3+}(500 μM) in the presence of 100-fold diluted human blood plasma spiked with different concentrations of ATP (0, 20, 50, 100 and 150 μM). (c, d) The corresponding relationship between (P-P_0) and the concentration of spiked ATP in the two human blood plasma samples.